Journal of Guidance, Control, and Dynamics,
Volume 45, Number 11, November 2022, pp. 2174–2181
DOI:10.2514/1.G006775

Nonlinear Analysis for Wing Rock System with Adaptive Control

Dongyang Li*
Nanjing University of Science and Technology, Nanjing 210094, China
Cranfield University, Cranfield MK43 0AL, UK

Antonios Tsourdos†
Cranfield University, Cranfield MK43 0AL, UK

Zhongyuan Wang‡
Nanjing University of Science and Technology, Nanjing 210094, China

Dmitry Ignatyev§
Cranfield University, Cranfield MK43 0AL, UK

I. Introduction

The potential of adaptive control in improving the performance and reliability of control systems attracts researchers and engineers from different disciplines. However, the verification and validation of the flight control system regarding modeling error, uncertainty, disturbance, and time delay is not an easy task due to the inherent nonlinearity of the problem as well as the lack of rigorous analysis tools for nonlinear systems [1–5].

Currently, to design a closed-loop system and to assess its stability and performance characteristics, well-developed linear analysis tools are used. For clearance of flight control laws, testing system capabilities in the worst-case scenario [6], bifurcation methods [7,8], and robust control techniques [9] are used. However, the majority of the techniques require linearization of system dynamics. The gap between linear analysis and nonlinear systems can cause undetected behavior of the system. Monte Carlo simulations of high-fidelity models could be utilized as a supplementary tool to analyze the viable subset of the flight envelope to prevent possible instability or violation of predefined constraints [10]. Even though the Monte-Carlo simulations could provide additional insight into the system dynamics, this approach is time-consuming and computationally expensive and cannot issue a stability certificate. In lieu of Monte Carlo simulations, sum-of-squares (SOS) programming techniques [11] provide an algebraic approach

Presented as Paper AIAA 2022-0691 at the AIAA SCITECH 2022 Forum, San Diego, CA & Virtual, January 3-7, 2022.
* PhD student, School of Energy and Power Engineering.
† Professor, School of Aerospace, Transport and Manufacturing, AIAA Senior Member.
‡ Professor, School of Energy and Power Engineering.
§ Senior Research Fellow, School of Aerospace, Transport and Manufacturing.

to the problem of nonlinear control analysis [10]. In recent years, a lot of research based on the SOS techniques for nonlinear analysis has been done for computing region of attraction (ROA), reachability sets, input-output gains, time delay margins, and robustness to uncertainty for nonlinear polynomial systems [12–15]. Based on the Lyapunov stability theory, a systematic approach employing SOS programming is developed to provide a deterministic estimation of the ROA [11]. This numerical method broadens the application of the analytical Lyapunov theory and has been modified for an improved estimation ever since [16–18]. It has been applied for the investigation of the aircraft control system, for instance, the F/A-18 falling-leaf mode control [19] and the control synthesis for deep-stall recovery [10]. A simple procedure for estimating the ROA of an adaptive control system is used in [20].

Although the SOS procedure can only accommodate dynamics described by polynomial vector fields, which has hitherto limited its applicability to, for instance, aeronautical control problems, it provides great potential to bridge the gap in the flight control validation process [19,21]. The clearance of adaptive strategies is an even more challenging task. Most of the adaptive algorithms make a closed-loop system a nonlinear one, and thus most of the analysis methods become inapplicable. Currently, the stability proofs for adaptive control systems are mostly obtained theoretically via selecting a Lyapunov function. However, this approach suffers from the ambiguity of the Lyapunov function determination and cannot be used to predict the real behavior of the system or validate the system's stability. From a practical point of view, measurable metrics are required to evaluate adaptive control systems. Some researchers tried to address this problem, in particular, the linear control notions of gain and phase margin are extended to the adaptive control flight system [1], and time delay margin[5,22] and input-output gains [15] for an adaptive control system are investigated theoretically or by using SOS programming. A relatively systematic overview of available robustness and performance metrics for adaptive flight control is provided in [23]. However, the lack of a universal approach and measurable metrics for adaptive control system validation still limits their wide usage.

The objective of this paper is to address the gap in analyzing adaptive control systems and to bring a new measurable metric for stability evaluation of adaptive control systems. This paper is focused more on the clearance of adaptive control laws rather than on design. In particular, we propose to utilize a numerical ROA estimate method to issue stability certificates. The region of attraction (ROA) of a locally asymptotically stable equilibrium point is an invariant set that all trajectories starting inside will converge to the equilibrium point [16]. It defines the region where a control system can operate safely and effectively, the estimation error bounds, and, thus, the uncertainty level. For a successful control design, the operational region of the system has to be ensured inside the ROA [24] and the uncertainty level has to be inside the estimation error bounds. A key element in adaptive control design is the tuning of hyperparameters, which obviously affects the system performance as well as the stability. One of the main performances of the adaptive system is a fast adaptation. This paper proposes a tool for studying the influence of the hyperparameters, such as the adaptation gain and the stability-enhancing σ-modification term, on the stability of the system through the numerical ROA estimation.

In this paper, we used a wing-rock benchmark model for validation of our approach. Wing rock is a well-known lateral-directional instability that occurs in aircraft of varying configurations and aspect ratios at a moderate to high angle of attack[25]. In this paper, wing rock augmented with a model reference adaptive control (MRAC) is taken as for demonstration of the proposed approach.

The paper is organized as follows. Firstly, the wing rock dynamics and the classical adaptive controller is described in Sec. II. In Sec. III, the algorithms for ROA estimation using SOS polynomial optimization are presented. Sec. IV summarizes the results of ROA analysis for an adaptive control system with respect to adaptation gain and sigma modification parameters. A discussion is followed in Sec. V and finally, the paper concludes in Sec. VI.

II. Wing Rock Dynamics and Adaptive Control

A. Wing Rock Model

The wing rock model has gained great attention and interest in the field of the aviation industry and serves as a classical benchmark example for the demonstration of various control methodologies [20]. Mathematical models of wing rock have been developed and the existence of limit cycle oscillations has been examined [25–27]. However, the aerodynamic rolling moment is a complex nonlinear function of the roll angle, roll rate, angle of attack, and sideslip angle, and its exact analytical expression is difficult to derive [28]. Even though the wing rock model was well elaborated, in real flight, the aerodynamic coefficients at high angles of attack can differ significantly from the model ones [29]. The model of wing rock, taken from [25], considering a flat, thin wing is constrained such that it is free only to roll about its x-axis, is described as

$$\ddot{\phi} = (\rho U_{\infty}{}^{2} Sb / 2I_{xx}C_{l}) + d_{0}u \tag{1}$$

where ϕ is the roll angle and the overdot denotes the time derivative. Also, ρ is the air density, U_{∞} is the speed of freestream, S is the reference wing area, b is the chord, I_{xx} is the mass moment of inertia of the wing around the midspan axis, and C_l is the roll-moment coefficient. Note that d_0 is the control effectiveness element, and the input signal u acts as part of the roll rate. The roll-moment coefficient is written as

$$C_l = a_1\phi + a_2\dot{\phi} + a_3\phi^3 + a_4\phi^2\dot{\phi} + a_5\phi\dot{\phi}^2 \tag{2}$$

The aerodynamic parameters a_i are nonlinear functions of the angle of attack which have been presented in [25]

Defining $\boldsymbol{x} = [x_1, x_2]^T = [\phi, \dot{\phi}]^T$, the wing rock system can be re-written as

$$\begin{cases} \dot{x}_1 = x_2 \\ \dot{x}_2 = f(\boldsymbol{x}) + d_0 u \end{cases} \tag{3}$$

where $\boldsymbol{x} \in \mathbb{R}^2$, the Euclidean space of dimension of two, and

$$f(\boldsymbol{x}) = \boldsymbol{b}^T \boldsymbol{h}(\boldsymbol{x}) \tag{4}$$

where

$$\begin{gathered} \boldsymbol{b} = [b_1, b_2, b_3, b_4, b_5]^T,\, b_i = (\rho U_\infty{}^2 Sb / 2I_{xx})a_i \quad i = 1,...,5 \\ \boldsymbol{h}(\boldsymbol{x}) = [x_1,\, x_2,\, x_1{}^3,\, x_1{}^2 x_2,\, x_1 x_2{}^2]^T \end{gathered} \tag{5}$$

B. Model Reference Adaptive Control

Approaches to suppress this unstable phenomenon have been explored [30–34]. To account for the uncertainty in the system, adaptive control is developed in [32,34,35]. A model reference adaptive controller applied to suppress the wing rock motion can be described as follows. The reference model carrying the desired response is given by

$$\dot{\boldsymbol{x}}_m = \boldsymbol{A}_m \boldsymbol{x}_m \tag{6}$$

where $\boldsymbol{x}_m = [x_{m1}, x_{m2}]^T$, $\varsigma > 0$, $\omega_n > 0$ and

$$\boldsymbol{A}_m = [0, 1; -\omega_n{}^2, -2\varsigma\omega_n] \tag{7}$$

where $\boldsymbol{A}_m$ is a Hurwitz matrix, and the reference trajectory asymptotically converges to zero as $t \to \infty$.

The wing rock control problem is formed under the assumption on $f(\boldsymbol{x})$: suppose that in Eq. (3) the parameters $b_i\,(i = 1, 2, ..., 5)$ and d_0 are unknown, but the sign of d_0 is known.

Defining the tracking error by $\boldsymbol{e} = [e_1, e_2]^T = \boldsymbol{x} - \boldsymbol{x}_m$ and

$$\dot{\boldsymbol{e}} = \boldsymbol{A}_m \boldsymbol{e} + \boldsymbol{d}_m[(\boldsymbol{b} - \boldsymbol{b}_m)^T \boldsymbol{h}(\boldsymbol{x}) + d_0 u] \tag{8}$$

where $\boldsymbol{d}_m = [0, 1]^T$ and $\boldsymbol{b}_m = [-\omega_n{}^2, -2\varsigma\omega_n, 0, 0, 0]^T$. If we define

$$\boldsymbol{\theta}^* = (\boldsymbol{b} - \boldsymbol{b}_m) / d_0 \tag{9}$$

as the uncertainty of the dynamic system, then an adaptive control law of the form

$$u = -\boldsymbol{\theta}^T \boldsymbol{h}(\boldsymbol{x}) \tag{10}$$

is designed with $\boldsymbol{\theta} = [\theta_1, \theta_2, \theta_3, \theta_4, \theta_5]^T$ as an estimate of the actual $\boldsymbol{\theta}^*$, which enables the control input to cancel out the system uncertainty. In this case, Eq. (8) becomes

$$\dot{\boldsymbol{e}} = \boldsymbol{A}_m \boldsymbol{e} + \boldsymbol{d}_m \tilde{\boldsymbol{\theta}}^T \boldsymbol{h}(\boldsymbol{x}), \quad \tilde{\boldsymbol{\theta}} = \boldsymbol{\theta}^* - \boldsymbol{\theta} \tag{11}$$

For the derivation of the adaptation law for $\tilde{\boldsymbol{\theta}}$, the Lyapunov approach is used but the details are omitted here due to the space limitation, and readers are referred to [28] for more information. Since $\dot{\tilde{\boldsymbol{\theta}}} = -\dot{\boldsymbol{\theta}}$, the adaptation law adjusting the parameter $\boldsymbol{\theta}$ is

$$\dot{\boldsymbol{\theta}} = \mathrm{sgn}(d_0)\boldsymbol{\Gamma}(\boldsymbol{e}^T \boldsymbol{P} \boldsymbol{d}_m)\boldsymbol{h}(\boldsymbol{x}) - \kappa_R \boldsymbol{\Gamma}\boldsymbol{\theta} \tag{12}$$

where the adaptation gain $\boldsymbol{\Gamma} = \mathrm{diag}(\Gamma_i)\ (i = 1,...,5)$ with $\Gamma_i > 0$. The latter term involving κ_R is a sigma modification term. $\boldsymbol{\Gamma}$ and κ_R are two important hyperparameters to be tuned while designing the adaptive control system. The adaptation gain $\boldsymbol{\Gamma}$ determines the main characteristics of the adaptive control system, namely, how quickly the adaptation parameter $\boldsymbol{\theta}$ evolves. For $\kappa_R > 0$, the sigma modification term helps to prevent the parameter drift by ensuring $\boldsymbol{\theta}$ uniformly bounded, which enhances the robustness of the system. It improves the robustness of the adaptive control system by removing the purely integral action of the adaptive law [36,37]. $\boldsymbol{P}$ is the positive definite solution of the Lyapunov equation

$$\boldsymbol{A}^T \boldsymbol{P} + \boldsymbol{P}\boldsymbol{A} = -\boldsymbol{Q}, \ \boldsymbol{Q} > 0 \tag{13}$$

where $\boldsymbol{A} = \boldsymbol{A}_m$. It has been proven that all error signals can be asymptotically stable [28,34].

C. Disturbed Wing Rock System with Adaptive Control

The implementation of controllers must be verified and validated under certain circumstances including modeling error, time delay, uncertainty, and disturbance. In terms of disturbance, a common scenario where the signal measurement process inevitably interferes is considered. The uncertainty is then introduced during the measurement of roll angle ϕ and roll rate $\dot{\phi}$. It was found that aerodynamic damping could depend nonlinearly on the angular rates and their derivatives and a polynomial description of these dependencies was used in [38,39]. Here, we follow the same approach and assume that there is an unmodelled uncertainty d_d, which has a quadratic dependency on the angular rate derivative

$$d_d = \mu x_2^{\,2} \tag{14}$$

where the constant μ indicates the level of the disturbance.

The disturbed measurement signals are written as

$$\boldsymbol{x}_d = [x_{1d}, x_{2d}]^T = [x_1 + d_d, x_2 + d_d]^T, \tag{15}$$

which is used to construct the control input signal

$$u_d = -\boldsymbol{\theta}^T \boldsymbol{h}_d(\boldsymbol{x}_d) \tag{16}$$

where u_d is the actual signal sent to the executing agent, and $\boldsymbol{h}_d$ is the relevant five-vector function. In this case, the actual adaptation law applied to the wing rock system becomes

$$\dot{\boldsymbol{\theta}} = -\operatorname{sgn}(d_0)\boldsymbol{\Gamma}(\boldsymbol{e}^T \boldsymbol{P}\boldsymbol{d}_m)\boldsymbol{h}_d(\boldsymbol{x}_d) - \kappa_R \boldsymbol{\Gamma}\boldsymbol{\theta} \tag{17}$$

and the error dynamics

$$\dot{\boldsymbol{e}} = \boldsymbol{A}_m \boldsymbol{e} + \boldsymbol{d}_m\{d_0 \tilde{\boldsymbol{\theta}} \boldsymbol{h}_d(\boldsymbol{x}_d) + (d_0\boldsymbol{\theta} - \boldsymbol{b}_m)^T[\boldsymbol{h}(x) - \boldsymbol{h}_d(\boldsymbol{x}_d)]\} \tag{18}$$

It can be seen that the control input does not cancel the effect of the uncertainty so the system cannot guarantee asymptotical stability. ROA estimation would help to evaluate whether the operating range is still within the system stability region and provide confidence in the controller implementation.

In the simulation, the aerodynamic parameters of an 80 deg delta wing at a 25 deg angle of attack [28] are used to demonstrate the wing rock motion. A model aircraft with $U_\infty = 15\text{m/s}$ and $b = 0.429\text{m}$ is employed. In this simulation study, the non-dimensional time $t^* = (4U_\infty/b)t$ is used as an independent variable with $4U_\infty/b = 139.86\,\text{s}^{-1}$ and thus $\dot{\boldsymbol{x}}$ is replaced by $\boldsymbol{x}'$ that represents the derivative with respect to t^* [28]. The time scaling using t^* is used to reduce the discrepancy between ϕ and $\dot{\phi}$ and to avoid the possible numerical issues. The parameters of the vector $\boldsymbol{b}$ representing the model (4) for the non-dimensional time t^* are listed below

$$b_1 = -0.02012844, \quad b_2 = 0.01051916$$
$$b_3 = 0.02596236, \quad b_4 = -0.1273338, \quad b_5 = 0.5197074$$
$$d_0 = 1$$

The open-loop system (3) with $u = 0$ was simulated for three initial conditions: A: $\phi(0) = 6$ deg, $\dot{\phi}(0) = 419.4$ deg/s, B: $\phi(0) = 30$ deg, $\dot{\phi}(0) = 1398$ deg/s, and C: $\phi(0) = 140$ deg, $\dot{\phi}(0) = 0$ deg/s. The phase plot in Fig. 1 shows the occurrence of wing rock at the small initial condition. For proper scaling of the results, the roll rate derivative is given for the non-dimensional time t^* with the corresponding scaling factor. The roll angle diverges for the latter two larger initial conditions. Then model reference adaptive control is introduced with adaptation gain $\Gamma_i = 15$ and $\kappa_R = 1$. The desired damping ς and natural frequency ω_n are 0.707 and 0.5, respectively. The reference signal is chosen as zero. For simplicity, $\boldsymbol{\theta}_0$ is set zero in the control law (10). As shown in Fig. 2 a) and b) the blue lines, the wing rock phenomenon is successfully suppressed and $\boldsymbol{\theta}$ converges to zero (for simplicity, only θ_1 is illustrated) for all three initial conditions A, B, and C. After introducing the disturbance, whose level μ is specified to take the value of 0.1. Simulation of the responses (red lines in Fig. 2) tells that the adaptive control is still effective for A and B but fails for C. For initial conditions C, the adaptive control cannot bring the roll angle to zero, and the roll angle and $\boldsymbol{\theta}$ all go to infinity. So it is interesting to figure out in which range the adaptive control keeps effective and how the control parameters, adaptation gain $\boldsymbol{\Gamma}$, and sigma modification value κ_R, affects the stable range of the control system. This may give some insights into the control design.

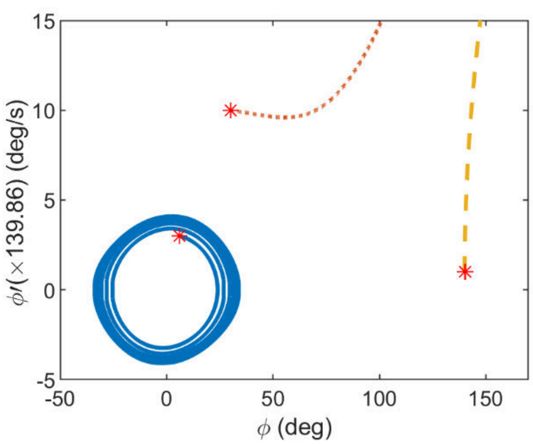

Fig. 1 Phase portrait for the open-loop wing rock system with non-dimensional time t^* (the red "✳" marks the initial condition).

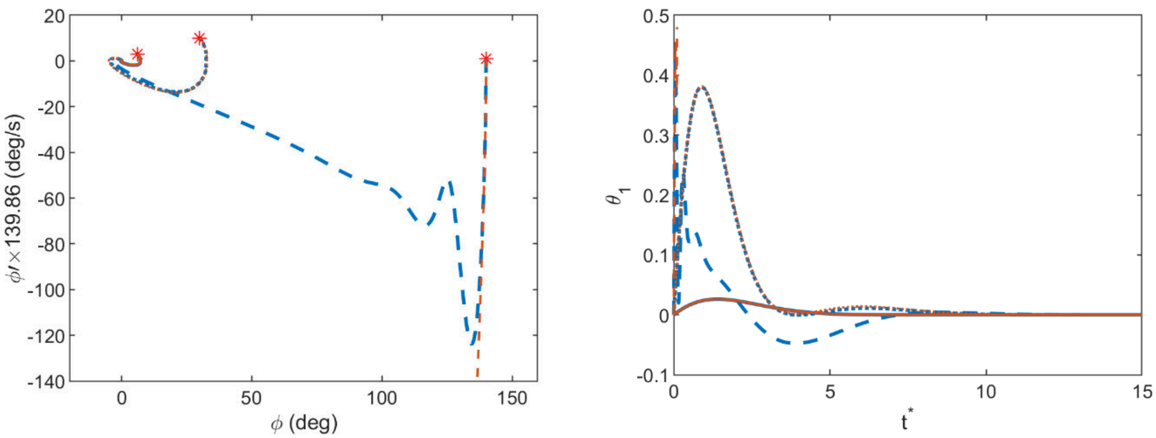

a) b)

Fig. 2 Adaptive wing rock system with (red) and without (blue) disturbance: a) phase plot; b) adaptation parameter θ_1 with non-dimensional time t^*. The red "✳" marks the initial conditions.

III.Region of Attraction Estimation

Consider an autonomous nonlinear polynomial system of the form

$$\dot{\boldsymbol{x}} = F(\boldsymbol{x}), \quad \boldsymbol{x}(0) = \boldsymbol{x}_0 \tag{19}$$

with $\boldsymbol{x} \in \mathbb{R}^n$ and $F(\boldsymbol{x})$ is a $n \times 1$ polynomial vector field. Without loss of generality, we assume that the origin is an asymptotically stable equilibrium point such that $F(0) = 0$. The ROA, a set of initial conditions whose trajectories will always converge back to the origin, can be defined as

$$\Omega := \left\{ \boldsymbol{x}_0 \in \mathbb{R}^n : \text{If } \boldsymbol{x}(0) = \boldsymbol{x}_0 \text{ then } \lim_{t \to \infty} \boldsymbol{x}(t) = 0 \right\} \tag{20}$$

Then the direct Lyapunov theory [11,40] is used to approximate the region of attraction by finding a Lyapunov function with a proper level set.

Lemma 1[11,40] If there exist a continuously differentiable scalar function $V(\boldsymbol{x}) : \mathbb{R}^n \to \mathbb{R}$ and a positive scalar $\gamma \in \mathbb{R}^+$, such that

$$V(\boldsymbol{x}) > 0 \quad \forall \boldsymbol{x} \neq 0 \text{ and } V(0) = 0 \tag{21}$$

$$\Omega := \{ \boldsymbol{x} : V(\boldsymbol{x}) < \gamma \} \text{ is bounded} \tag{22}$$

$$\Omega \subseteq \{ \boldsymbol{x} : (\partial V / \partial \boldsymbol{x}) F < 0 \} \bigcup \{0\} \tag{23}$$

then the origin is asymptotically stable and Ω_γ is a subset of the ROA. $V(\boldsymbol{x})$ is the so-called local Lyapunov function.

As can be seen, set containment constraints are involved in Eqs. (21)-(23) so the well-known generalized S-procedure [41] is employed to provide sufficient conditions for them to be represented by inequalities that are then treatable by the SOS procedure.

Lemma 2 (Generalized S-procedure [41]). Given polynomials $g_0(\boldsymbol{x}),...,g_m(\boldsymbol{x}) \in \boldsymbol{R}[\boldsymbol{x}]$ and polynomials

$$s_1(\boldsymbol{x}),...,s_m(\boldsymbol{x}) \in \Sigma_n$$

if

$$g_0(\boldsymbol{x}) - \sum_{i=1}^{m} s_i(\boldsymbol{x}) g_i(\boldsymbol{x}) \geq 0 \tag{24}$$

then

$$\left\{\boldsymbol{x} \in \mathbb{R}^n : g_1(\boldsymbol{x}),...,g_m(\boldsymbol{x}) \geq 0\right\} \subseteq \left\{\boldsymbol{x} \in \mathbb{R}^n : g_0(\boldsymbol{x}) \geq 0\right\} \tag{25}$$

where $\boldsymbol{R}[\boldsymbol{x}]$ represents the set of polynomials in $\boldsymbol{x} \in \mathbb{R}^n$ with real coefficients and Σ_n denotes the set of the sum of squares polynomials in $\boldsymbol{x} \in \mathbb{R}^n$.

With a polynomial dynamic system and under the assumption of a polynomial Lyapunov function V, the ROA estimation problem in Eqs. (21)-(23) can be described by polynomial inequalities. Using the SOS procedure, these inequalities are represented as a sum of squares. The ROA estimation problem is then formulated by a SOS problem

$$\begin{gathered} \max \ \gamma \\ \text{Subject to}: -[(\partial V / \partial \boldsymbol{x}) F + l_1] - (\gamma - V) s_1 \in \Sigma_n \end{gathered} \tag{26}$$

where l_1 is a positive polynomial (typically $\varepsilon \boldsymbol{x}^T \boldsymbol{x}$ with some small real number ε) which is used to guarantee the derivative of V to be strictly negative. $s_1(\boldsymbol{x})$ is a decision SOS multiplier with a proper degree. Σ_n denotes the set of SOS polynomials in $\boldsymbol{x} \in \mathbb{R}^n$. The optimized γ provides a guaranteed lower bound for the ROA. Since the optimization variable γ is coupled with s_1, the bisection procedure is required to find the maximum γ of a fixed V. A proper choice of s_1 is important to capture the feasible result of the problem described by Eq. (26) without introducing an unnecessary computation burden. According to [42], its degree can be chosen by

$$\begin{gathered} \max D(V\, s_1) \geq \max D((\partial V / \partial \boldsymbol{x}) F + l_1) \\ \min D(s_1) \geq \min D((\partial V / \partial \boldsymbol{x}) F + l_1) \end{gathered} \tag{27}$$

where $D(\cdot)$ represents the degree of a polynomial. The freely available toolboxes SOSOPTs and solver SeDuMi [21], are used in this Note to solve the problem. Readers are referred to [41] for more information about the SOS programming and the toolboxes.

The result can be conservative because of many reasons, for example, the shape of the Lyapunov function, the SOS relaxation procedure, and the set containment treatment. Then exhaustive Monte Carlo search is carried out using $\theta_i = 0\ (i = 1,...,5)$ to give an insight into the upper bound of ROA on the $\phi - \dot{\phi}$ plane, which helps to evaluate the extent to which the estimation obtained using the SOS approach is conservative.

IV.Results

As it was mentioned earlier, one of the main characteristics of the adaptive control system is the capability of fast adaptation. The MRAC performance can be optimized by tuning the hyperparameters, namely, the adaptation rate $\boldsymbol{\Gamma}$ and the sigma modification κ_R. One important step in verifying the adaptive control law is to ensure that the operational region of the system is contained in the ROA. The disturbed adaptive control model in Eqn. (17) and (18) can have an altered ROA compared with the original system. In this section, the ROAs for different values of the adaptation rate $\boldsymbol{\Gamma}$ and the sigma modification term κ_R are analyzed.

Linearization analysis shows that the origin is an asymptotically stable equilibrium point of the disturbed wing rock control system. To initialize the bisection procedure for estimation, a second-order Lyapunov function is computed as

$$V = \boldsymbol{x}^T \boldsymbol{P} \boldsymbol{x} + \boldsymbol{\theta}^T \boldsymbol{\Gamma}^{-1} \boldsymbol{\theta} \tag{28}$$

where $\boldsymbol{P}$ is determined by Eq. (13) with $\boldsymbol{Q} = \boldsymbol{I}$ ($\boldsymbol{I}$ is the unit matrix) and $\boldsymbol{P} = [2.298, 2.000; 2.000, 3.536]$ in this example; $\boldsymbol{\Gamma} = \Gamma \boldsymbol{I}$, and Γ is a positive scalar which is an important control design parameter.

A. Adaptation Rate

The effect of varying adaptation rates is explored by analyzing the ROA with respect to the origin of the disturbed adaptive system. In this case, the sigma modification value is held constant as 1 to isolate the effect of a changing adaptation rate. The largest possible values of the level sets for the Lyapunov function (28) is searched by the SOS procedure and the results are given in Table 1. The discrepancy in these values is small. However, Γ variation has a more tangible effect on the ROA, which is analyzed through 2D cross-sections of the ROA estimates in Fig. 3. The bounds on $\theta_i (i = 1, 2, ..., 5)$ increase as Γ increases. This makes sense because a larger adaptation rate enhances the adaptive law and a smaller adaptation rate disables the adaptive law [5]. The numeric simulation validates that the trajectory converges to zero when Γ =10 but diverges when Γ =1 at $\phi = 5$ deg, $\dot{\phi} = 0$, $\theta_2 = -15$ and zero initial values for other adaptation variables.

Table 1 Level set of Lyapunov functions for different adaptation rates

Γ	Level set of V in Eq. (28)
0.01	2.09180
0.1	2.07031
1	2.05261
10	2.04883
100	2.04883
1000	2.04863

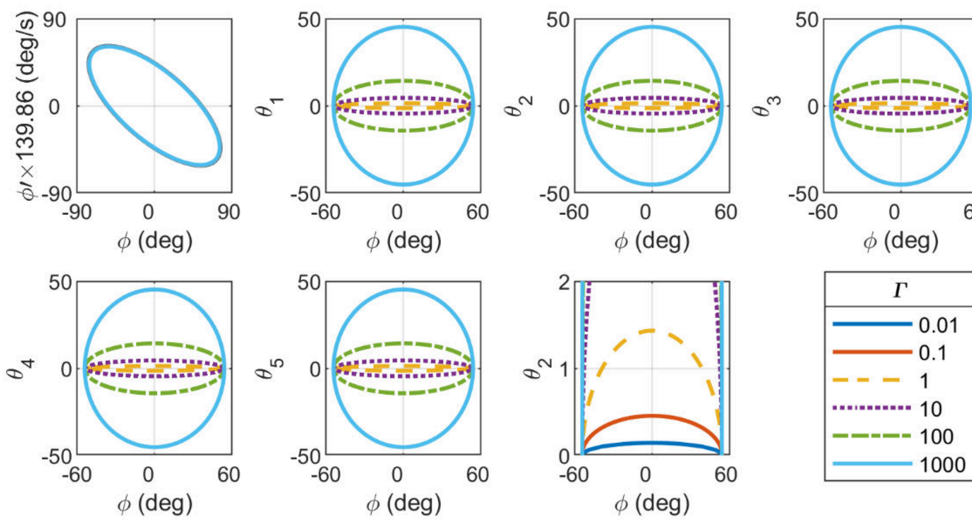

Fig. 3 Estimated ROA for different adaptation rates.

B. Sigma Modification

Similarly, the effect of varying sigma modification values κ_R on the MRAC closed-loop system under proposed conditions is explored with the adaptation rate Γ fixed at 1. The sigma modification is used to prevent parameter drift by bounding the evolution of estimation parameters. By analyzing the region of attraction around the origin, the largest possible values for the level set of the Lyapunov function $V = \boldsymbol{x}^T \boldsymbol{P} \boldsymbol{x} + \boldsymbol{\theta}^T \boldsymbol{\theta}$ are obtained, as shown in Table 2. Again, 2D cross-sections of ROA for different values of κ_R are used for analysis, which is demonstrated in Fig. 4. These results manifest that κ_R also affects the ROA size, however, it is less as compared to Γ . Similarly, the numerical simulation validates that the trajectory converges to zero when κ_R =10 but diverges when κ_R =1 at $\phi = 5$ deg, $\dot{\phi} = 0$, $\theta_2 = -15$ and zero initial values for other adaptation variables. The trajectory simulation in Fig. 5

shows that the larger the sigma modification value, the faster the convergence and the smaller the overshoot for the adaptation parameters, thus a larger range of initial conditions can be stabilized. The illustrative results of the SOS method in Fig. 4 support this statement.

Table 2 Level set of Lyapunov function for different sigma modification values

κ_R	**Level set of V in Eq. (28)**
0.01	1.68945
0.1	1.86230
1	2.05261
10	2.09351
100	2.09863
1000	2.09863

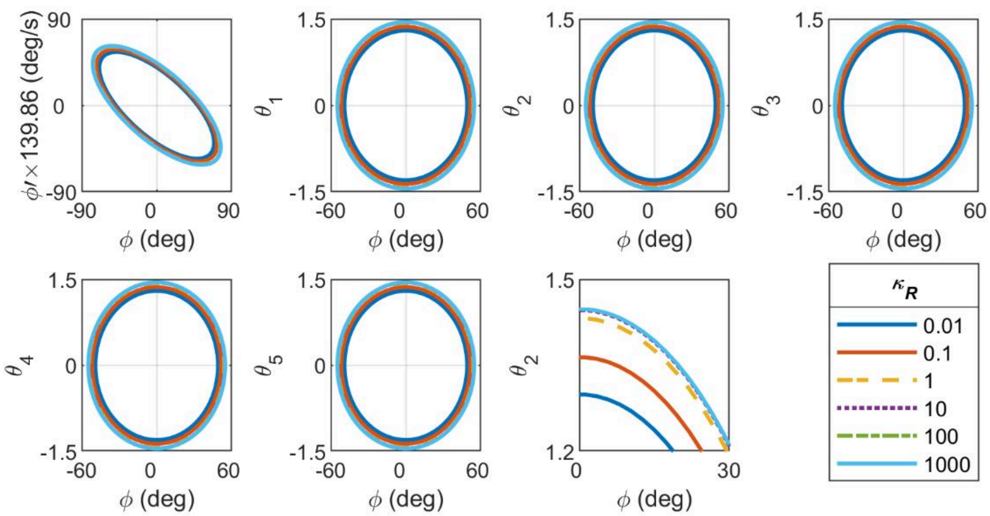

Fig. 4 Estimated ROA for different sigma modification values.

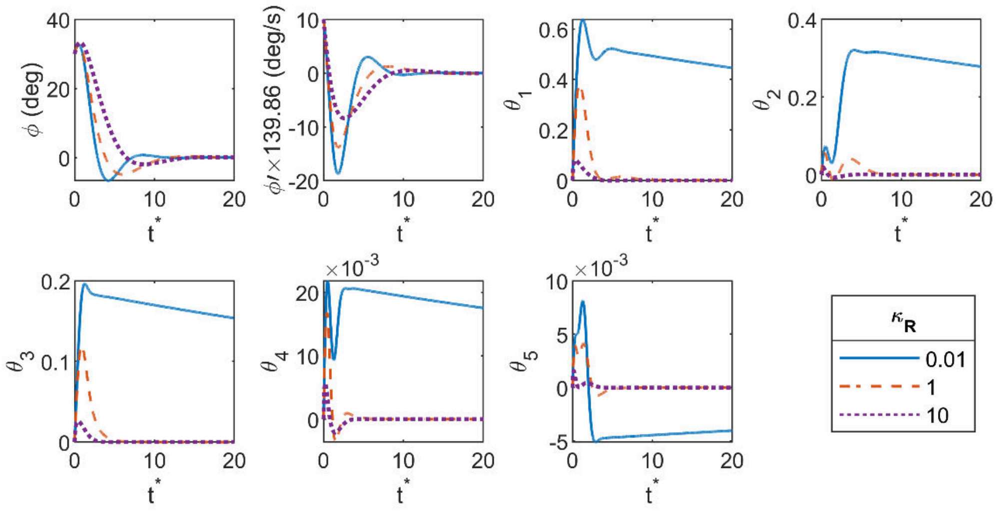

Fig. 5 Variables evolution for different sigma modification values.

The SOS results above imply that the ROA for $\boldsymbol{\theta}$ grows with the increase of both adaptation rate and sigma modification value. A larger value of both the control parameters can assure a larger set of stable initial conditions, and adaptive parameters have a larger upper bound.

V.Discussion

The proposed approach for analysis of the hyper parameters, the adaptation gain Γ and the modification term value κ_R, allows proper selection of adaptation gain. Taking into account that the SOS technique was shown to be a useful tool for time-delay margin [5,22] and input-output gain [15] analysis, SOS provides a comprehensive tool for adaptive control system design.

For validation purposes, Monte Carlo simulations are performed on a boxed area of $\phi \in [-360, 360]\text{deg}$ and $\dot{\phi} \in [-540\times 139.86, 540\times 139.86]\text{deg/ s}$, and stable initial conditions on the $\phi - \dot{\phi}$ plane are obtained, as shown in the upper right area encircled by the curves in Fig. 6. The results indicate that the ROA is sensitive to the control parameter Γ and κ_R, and the variation with Γ is relatively more obvious than that with κ_R. This confirms the results obtained by the SOS procedure in Fig. 3 and Fig. 4.

At the same time, the ROA estimates by SOS procedures are also demonstrated along with the Monte Carlo results as shown in Fig. 6, which reveals some limitations of the current method because of the usage of elliptical shapes (i.e. quadratic Lyapunov functions) to estimate the ROA. However, in our high-dimensional case, the ROA has a more complex shape, and thus algorithm yields more conservative estimates. In order to overcome these limitations, methods using other more complex shapes, namely, high-order Lyapunov functions or superimposing elliptical shapes, might be useful.

It is an inherent limitation of the SOS optimization that it is sensitive to both the state order and the polynomial degree of the model. The formulation of the ROA estimation problem results in a total of seven states and six-degree polynomials describing each variable. Considering that the size of the problem has approached the upper limit of SOS optimization, only a second-order Lyapunov function as in Eqn. (28) is evaluated, which takes two hours for one iteration in the bisection sequence with a 16-core processor and 12G of RAM. About 10-20 iterations are needed to obtain the level set in Table 1 and Table 2 with a tolerance of 1e-4. A higher-order Lyapunov function can further enlarge the SOS program in principle but for an adaptive control system, a large number of estimation parameters θ_i can easily inflate the SOS program, which can result in a shortage of available memory and computation power [5].

Another limitation of SOS optimization is its reliance on polynomial models. Proper polynomial approximation [43] and piecewise polynomial models for a complex model (for example, the aerodynamic coefficients at the low and high angle of attack across the flight envelope) [10] have been proposed to work around this limit. The computation has also been extended to rational and composite Lyapunov functions [13]. Numerical computation is also sensitive to the dynamics of the systems. Time scalings can be used to preprocess the problem and reduce numerical issues [5].

Even though the estimated ROA is still less than the ROA estimate via Monte Carlo and the controller design based on it might be too conservative, the estimation results cover the majority of the operational domain and provide a solid ground for adaptive control system exploitation domain.

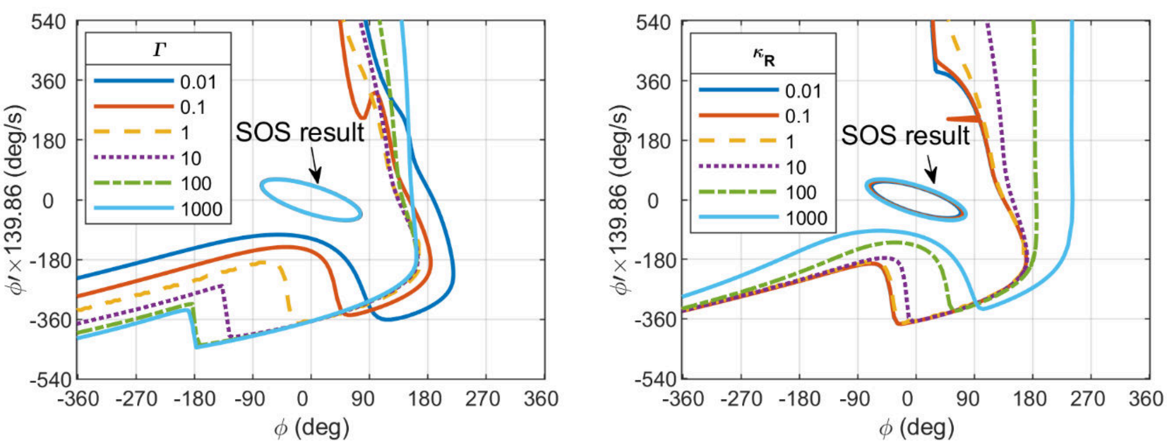

Fig. 6 Upper bound of ROA obtained by Monte Carlo simulations

VI. Conclusion

The lack of rigorous numerical techniques for the clearance of adaptive control systems is one of the obstacles preventing the wide usage of these promising techniques. Most of the adaptive algorithms make a closed-loop system a nonlinear one, and thus most of the classical control design and clearance methods become inapplicable. This paper proposes novel measurable metrics for adaptive control stability evaluation. In particular, it is proposed to use a numerical region-of-attraction estimate to issue stability certificates. A key element in adaptive control design is the tuning of hyperparameters, which affects the system performance as well as the stability. One of the main performances of the adaptive system is a fast adaptation. The approach is demonstrated through the investigation of the influence of these hyperparameters, such as adaptation gain and the stability-enhancing σ-modification term, on the stability of the system through the numerical ROA estimates. The ROA is estimated using the sum of squares (SOS) optimization technique. The benchmark model of wing rock dynamics with a model reference adaptive control is utilized for validation purposes.

The performed analysis manifests that the performance of the adaptive control system might be improved for larger adaptive gains since the system can adapt to unknown dynamics faster and can accommodate larger adaptation gain error bounds. Larger values of sigma modifications also improve the performance of the system, namely, decreasing overshoots and increasing the stable region of initial conditions.

The analysis of results shows some limitations of the current method because of the usage of elliptical shapes to cover the ROA. For highly nonlinear systems with a large number of states, the ROAs have complex shapes, and thus algorithm yields more conservative estimations. Even though the estimated ROA is still less than the Monte-Carlo-based ones, the results from the SOS optimization cover the majority of the operational domain and provide a solid ground for the adaptive control system exploitation domain.

References

[1] Dydek, Z. T., Jain, H., Jinho, J., Annaswamy, A. A. M., Lavretsky, E., Jang, J., Annaswamy, A. A. M., and Lavretsky, E. “Theoretically Verifiable Stability Margins for an Adaptive Controller,” *AIAA Guidance, Navigation, and Control Conference 2006*, Vol. 5, American Institute of Aeronautics and Astronautics, Keystone, Colorado, 2006, pp. 2821–2834. https://doi.org/10.2514/6.2006-6416.

[2] Chandramohan, R., and Calise, A. J. "Output Feedback Adaptive Control of Plants with Unmodeled Dynamics and Input Uncertainties." *Journal of Guidance, Control, and Dynamics*, Vol. 42, No. 10, 2019, pp. 2143–2156. https://doi.org/10.2514/1.G003548.

[3] Dobrokhodov, V., Kaminer, I., Kitsios, I., Xargay, E., Hovakimyan, N., Cao, C., Gregory, I. M., and Valavani, L. "Experimental Validation of L1 Adaptive Control: The Rohrs Counterexample in Flight." *Journal of Guidance, Control, and Dynamics*, Vol. 34, No. 5, 2011, pp. 1311–1328. https://doi.org/10.2514/1.50683.

[4] Jacklin, S., Schumann, J., Gupta, P., Lowry, M., Bosworth, J., Zavala, E., Hayhurst, K., Belcastro, C., and Belcastro, C. "Verification, Validation, and Certification Challenges for Adaptive Flight-Critical Control System Software," *AIAA Guidance, Navigation, and Control Conference and Exhibit*, Vol. 4, American Institute of Aeronautics and Astronautics, Reston, Virigina, 2004, pp. 2648–2657. https://doi.org/10.2514/6.2004-5258.

[5] Dorobantu, A., Seiler, P., and Balas, G. J. "Time-Delay Margin Analysis for an Adaptive Controller." *Journal of Guidance, Control, and Dynamics*, Vol. 35, No. 5, 2012, pp. 1418–1425. https://doi.org/10.2514/1.56719.

[6] Varga, A. "Optimisation-Based Clearance." In *Advanced Techniques for Clearance of Flight Control Laws* (C. Fielding, A. Varga, S. Bennani, and M. Selier, eds.), Springer Berlin Heidelberg, Berlin, Heidelberg, 2002, pp. 107–117.

[7] Goman, M. G., Zagainov, G. I., and Khramtsovsky, A. V. "Application of Bifurcation Methods to Nonlinear Flight Dynamics Problems." *Progress in Aerospace Sciences*, Vol. 33, Nos. 9–10, 1997, pp. 539–586. https://doi.org/10.1016/S0376-0421(97)00001-8.

[8] Lowenberg, M., and Richardson, T. "Bifurcation-Based Clearance of Linear Stability Criteria." In *Advanced Techniques for Clearance of Flight Control Laws*, Springer Berlin Heidelberg, Berlin, Heidelberg, 2002, pp. 355–383.

[9] Packard, A., Seiler, P., and Balas, G. "Structured Singular Value and Applications: Analyzing the Effect of Linear Time-Invariant Uncertainty in Linear Systems." In *Encyclopedia of Systems and Control*, Springer, London, 2014, pp. 1–8.

[10] Cunis, T., Condomines, J.-P., and Burlion, L. “Sum-of-Squares Flight Control Synthesis for Deep-Stall Recovery.” *Journal of Guidance, Control, and Dynamics*, Vol. 43, No. 8, 2020, pp. 1498–1511. https://doi.org/10.2514/1.G004753.

[11] Parrilo, P. A. “Structured Semidefinite Programs and Semialgebraic Geometry Methods in Robustness and Optimization.” California Institute of Technology, Pasadena, CA, 2000.

[12] Papachristodoulou, A., and Prajna, S. “A Tutorial on Sum of Squares Techniques for Systems Analysis,” *Proceedings of the 2005 American Control Conference*, Vol. 4, IEEE, Portland, OR, USA, 2005, pp. 2686–2700. https://doi.org/10.1109/ACC.2005.1470374.

[13] Cunis, T., Condomines, J.-P., and Burlion, L. “Local Stability Analysis for Large Polynomial Spline Systems.” *Automatica*, Vol. 113, 2020, pp. 1–5. https://doi.org/10.1016/j.automatica.2019.108773.

[14] Pandita, R., Chakraborty, A., Seiler, P., and Balas, G. “Reachability and Region of Attraction Analysis Applied to GTM Dynamic Flight Envelope Assessment,” *AIAA Guidance, Navigation, and Control Conference*, AIAA, Reston, Virigina, 2009. https://doi.org/10.2514/6.2009-6258.

[15] Dorobantu, A., Seiler, P., and Balas, G. “Nonlinear Analysis of Adaptive Flight Control Laws,” *AIAA Guidance, Navigation, and Control Conference*, AIAA, Toronto, Ontario, Canada, 2010. https://doi.org/10.2514/6.2010-8043.

[16] Khodadadi, L., Samadi, B., and Khaloozadeh, H. “Estimation of Region of Attraction for Polynomial Nonlinear Systems: A Numerical Method.” *ISA Transactions*, Vol. 53, No. 1, 2014, pp. 25–32. https://doi.org/10.1016/j.isatra.2013.08.005.

[17] Sidorov, E., and Zacksenhouse, M. “Lyapunov Based Estimation of the Basin of Attraction of Poincare Maps with Applications to Limit Cycle Walking.” *Nonlinear Analysis: Hybrid Systems*, Vol. 33, 2019, pp. 179–194. https://doi.org/10.1016/j.nahs.2019.03.002.

[18] Chen, Y.-J., Tanaka, M., Tanaka, K., and Wang, H. O. “Stability Analysis and Region-of-Attraction Estimation Using Piecewise Polynomial Lyapunov Functions: Polynomial Fuzzy Model Approach.” *IEEE Transactions on Fuzzy Systems*, Vol. 23, No. 4, 2015, pp. 1314–1322. https://doi.org/10.1109/TFUZZ.2014.2347993.

[19] Chakraborty, A., Seiler, P., and Balas, G. J. “Susceptibility of F/A-18 Flight Controllers to the Falling-Leaf Mode: Nonlinear Analysis.” *Journal of Guidance, Control, and Dynamics*, Vol. 34, No. 1, 2011, pp. 73–85. https://doi.org/10.2514/1.50675.

[20] Li, D., Ignatyev, D., Tsourdos, A., and Wang, Z. “Region of Attraction Analysis for Adaptive Control of Wing Rock System,” *3rd IFAC Conference on Modelling, Identification and Control of Nonlinear Systems MICNON 2021*, Vol. 54, Elsevier Ltd, Tokyo, Japan, 2021, pp. 518–523. https://doi.org/10.1016/j.ifacol.2021.10.407.

[21] Chakraborty, A., Seiler, P., and Balas, G. J. “Nonlinear Region of Attraction Analysis for Flight Control Verification and Validation.” *Control Engineering Practice*, Vol. 19, No. 4, 2011, pp. 335–345. https://doi.org/10.1016/j.conengprac.2010.12.001.

[22] Heise, C. D., and Holzapfel, F. “Time-Delay Margin Computation of Model Reference Adaptive Control Using the Razumikhin Theorem.” *Proceedings of the IEEE Conference on Decision and Control*, Vols. 2015-Febru, No. February, 2014, pp. 529–535. https://doi.org/10.1109/CDC.2014.7039435.

[23] Heise, C. D., Leitão, M., and Holzapfel, F. “Performance and Robustness Metrics for Adaptive Flight Control - Available Approaches.” *AIAA Guidance, Navigation, and Control (GNC) Conference*, No. August, 2013. https://doi.org/10.2514/6.2013-5090.

[24] Chakraborty, A., Seiler, P., and Balas, G. J. “Susceptibility of F/A-18 Flight Controllers to the Falling-Leaf Mode: Linear Analysis.” *Journal of Guidance, Control, and Dynamics*, Vol. 34, No. 1, 2011, pp. 57–72. https://doi.org/10.2514/1.50674.

[25] Nayfeh, A. H., Elzebda, J. M., and Mook, D. T. “Analytical Study of the Subsonic Wing-Rock Phenomenon for Slender Delta Wings.” *Journal of Aircraft*, Vol. 26, No. 9, 1989, pp. 805–809. https://doi.org/10.2514/3.45844.

[26] Chen, K., Dong, Y., Shi, Z., Tong, S. X., and Sha, J. “Experimental Study of the Suppression of Wing-Body Rock by Spanwise Blowing.” *2019 IEEE 10th International Conference on Mechanical and Aerospace Engineering, ICMAE 2019*, 2019, pp. 142–146. https://doi.org/10.1109/ICMAE.2019.8880951.

[27] Guglieri, G., and Quagliotti, F. B. “Analytical and Experimental Analysis of Wing Rock.” *Nonlinear Dynamics*, Vol. 24, No. 2, 2001, pp. 129–146. https://doi.org/https://link.springer.com/article/10.1023/A:1008328528873.

[28] Singh, S. N., Yirn, W., and Wells, W. R. "Direct Adaptive and Neural Control of Wing-Rock Motion of Slender Delta Wings." *Journal of Guidance, Control, and Dynamics*, Vol. 18, No. 1, 1995, pp. 25–30. https://doi.org/10.2514/3.56652.

[29] Ignatyev, D. I., Sidoryuk, M. E., Kolinko, K. A., and Khrabrov, A. N. "Dynamic Rig for Validation of Control Algorithms at High Angles of Attack." *Journal of Aircraft*, Vol. 54, No. 5, 2017, pp. 1760–1771. https://doi.org/10.2514/1.C034167.

[30] Cao, C., Hovakimyan, N., and Lavretsky, E. "Application of L1 Adaptive Controller to Wing Rock," *AIAA Guidance, Navigation, and Control Conference and Exhibit*, Vol. 5, American Institute of Aeronautics and Astronautics, Keystone, Colorado, 2006, pp. 2941–2952. https://doi.org/10.2514/6.2006-6426.

[31] Ignatyev, D. I., Zaripov, K. G., Sidoryuk, M. E., Kolinko, K. A., and Khrabrov, A. N. "Wind Tunnel Tests for Validation of Control Algorithms at High Angles of Attack Using Autonomous Aircraft Model Mounted in 3DOF Gimbals," *AIAA Atmospheric Flight Mechanics Conference*, Vol. 2016-Janua, American Institute of Aeronautics and Astronautics, Reston, Virginia, 2016, pp. 1–18. https://doi.org/10.2514/6.2016-3106.

[32] Malekzadeh, M., Sadati, J., and Alizadeh, M. "Adaptive PID Controller Design for Wing Rock Suppression Using Self-Recurrent Wavelet Neural Network Identifier." *Evolving Systems*, Vol. 7, No. 4, 2016, pp. 267–275. https://doi.org/10.1007/s12530-015-9143-3.

[33] Lee, K. W., and Singh, S. N. "Noncertainty-Equivalent Adaptive Wing-Rock Control via Chebyshev Neural Network." *Journal of Guidance, Control, and Dynamics*, Vol. 37, No. 1, 2014, pp. 123–133. https://doi.org/10.2514/1.61639.

[34] Calise, A. J., Shin, Y., and Johnson, M. D. "A Comparison Study of Classical and Neural Network Based Adaptive Control of Wing Rock." *AIAA Guidance, Navigation, and Control Conference*, Vol. 4, No. August, 2004, pp. 2728–2744. https://doi.org/10.2514/6.2004-5320.

[35] Sharma, B. B., and Kar, I. N. "Adaptive Control of Wing Rock System in Uncertain Environment Using Contraction Theory," *2008 American Control Conference*, IEEE, 2008, pp. 2963–2968. https://doi.org/10.1109/ACC.2008.4586946.

[36] Ioannou, P. A., and Kokotovic, P. V. "Robust Redesign of Adaptive Control." *IEEE Transactions on Automatic Control*, Vol. 29, No. 3, 1984, pp. 202–211. https://doi.org/10.1109/TAC.1984.1103490.

[37] Ioannou, P., and Fidan, B. “Adaptive Control Tutorial (Advances in Design and Control).” Society for Industrial and Applied Mathematics, 2007, pp. 62-67.

[38] Ignatyev, D. I., and Khrabrov, A. N. “Model of the Unsteady Aerodynamic Characteristics at High AOA with Nonlinear Dependency in Angular Rate,” *29th Congress of the International Council of the Aeronautical Sciences, ICAS 2014*, St. Petersburg, Russa, ICAS.org, Paper 0449, 2014.

[39] Ignatyev, D. I., Khrabrov, A. N., Kortukova, A. I., Alieva, D. A., Sidoryuk, M. E., and Bazhenov, S. G. “Interplay of Unsteady Aerodynamics and Flight Dynamics of Transport Aircraft in Icing Conditions.” *Aerospace Science and Technology*, Vol. 104, September 2020, Paper 105914. https://doi.org/10.1016/j.ast.2020.105914.

[40] Tan, W. “Nonlinear Control Analysis and Synthesis Using Sum-of-Squares Programming.” Berkeley: University of California, 2006.

[41] Topcu, U., and Packard, A. “Local Stability Analysis for Uncertain Nonlinear Systems.” *IEEE Transactions on Automatic Control*, Vol. 54, No. 5, 2009, pp. 1042–1047. https://doi.org/10.1109/TAC.2009.2017157.

[42] Tan, W., and Packard, A. “Stability Region Analysis Using Sum of Squares Programming,” *2006 American Control Conference*, IEEE, Minneapolis, MN, USA, 2006,pp. 2297-2302. https://doi.org/10.1109/ACC.2006.1656562.

[43] Sidoryuk, M. E., and Khrabrov, A. N. “Estimation of Regions of Attraction of Aircraft Spin Modes.” *Journal of Aircraft*, Vol. 56, No. 1, 2019, pp. 205–216. https://doi.org/10.2514/1.C034936.

2022-07-25

Nonlinear analysis for wing-rock system with adaptive control

Li, Dongyang

AIAA

Li D, Tsourdos A, Wang Z, Ignatyev D. (2022) Nonlinear analysis for wing-rock system with adaptive control. Journal of Guidance, Control, and Dynamics, Volume 45, Number 11,
þÿ N o v e m b e r 2 0 2 2 , p p . 2 1 7 4 2 1 8 1
https://doi.org/10.2514/1.G006775